2,9-Diazadibenzoperylene and 2,9-Dimethyldibenzoperylene-1,3,8,10-tetratriflates: Key to Functionalized 2,9-Diazaperopyrenes

Eduard Baal,[a] Marius Klein,[a] Klaus Harms,[a] and Jörg Sundermeyer*[a]

Abstract: The synthesis of 2,9-diaza-1,3,8,10-tetratriflato-dibenzoperylene (DDP **3a**) and corresponding 2,9-dimethyl-1,3,8,10-tetratriflato-dibenzoperylene (DBP **3b**) has been developed at multigram scale via reduction of one of the industrially most important high-performance dyes, perylene-3,4,9,10-tetracarboxylic diimide (PTCDI), and of the corresponding dihydroxy peropyrenequinone precursor. The focus of this paper is on the reactivity pattern of **3a** as key intermediate towards highly functionalized 2,9-diazadibenzopyrelenes (DDPs) obtained via catalytic substitution of four triflate by aryl, heteroaryl, alkynyl, aminyl, and O-phosphanyl substituents. The influence of electron-donating substituents (OSiMe$_3$, OP*t*-Bu$_2$, N-piperidinyl), electron-withdrawing (OTf, 3,5-bis-trifluoromethyl-phenyl), and of electron-rich π-conjugated (2-thienyl, 4-tert-butylphenyl, trimethylsilyl-ethynyl) substituents on optoelectronic and structural properties of these functionalized DDPs has been investigated via XRD analyses, UV/Vis, PL spectroscopy, and by electroanalytical CV. These results were correlated to results of DFT and TD-DFT calculations. Thus, functionalized DPPs with easily tunable HOMO and LUMO energies and gap became available via a new and reliable synthetic strategy starting from readily available PTCDI.

Introduction

Polycyclic (hetero)aromatic hydrocarbons (PAHs) are a versatile class of organic functional molecules investigated for their potential application in a number of technologies, such as organic photovoltaic devices (OPVs), organic field-effect transistors (OFETs) and energy storage applications.[1–12] Vast synthetic methodologies of their functionalization allow tailoring of their structural and optoelectronic properties. E.g., for the class of tetraazaperopyrenes (TAPP) related to our 2,9-diazaperopyrene title compounds (2,9-diazadibenzoperylenes, DDPs) an elaborate multi-step synthesis protocol was established in recent years.[11,12]

The probably most extensively studied and applied class of PAHs is derived from perylene-3,4,9,10-tetracarboxylic diimides (PDIs). The functionalization of PDIs is well established, but until now, PDIs photophysical and electrochemical properties were almost exclusively modified via substituents in the bay or *N*-diimide positions.[14–15]

The family of diazadibenzoperylenes (Figure 1) can be rationalized simply as products of PTCDI carbonyl group reduction. Nevertheless, only few reports of substituted or unsubstituted DDPs are known despite their structural relation to the archetypical PDIs.[16,17] The synthesis of DDPs was previously described in a two-step procedure via complete reduction of PTCDIs imide carbonyl groups to CH_2 functionalities, subsequently followed by oxidative aromatization to form unsubstituted and poorly soluble DDP.[18] The low solubility of unsubstituted DDP is a drawback with respect to its further functionalization. A simpler approach to unsubstituted DDP involves naphthalene and triazine as starting materials.[19] Previous studies on DDPs demonstrated their functionality as sigma-donor ligands in tetranuclear Pd^{2+} und Pt^{2+} metallacycles and macromolecular systems.[20] Other studies investigated the binding affinities of cationic *N*-alkylated DDPs to nucleotides,[18] their intercalation with

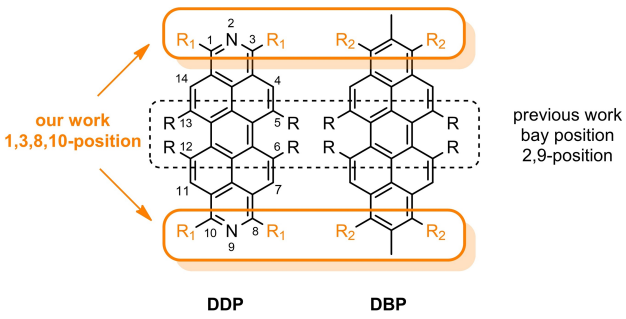

Figure 1. Functionalization sites of 2,9-diazadibenzoperylenes (DDP) and dibenzoperylenes (DBP) in 1-,3-, 8-, 10-positions described in our and previous work.[20,26]

[a] *Dr. E. Baal, M. Klein, Dr. K. Harms, Prof. Dr. J. Sundermeyer*
Chemistry Department and Materials Sciences Center
Philipps-Universität Marburg
Hans-Meerwein-Straße 4, 35032 Marburg (Germany)
E-mail: JSU@staff.uni-marburg.de

Supporting information for this article is available on the WWW under https://doi.org/10.1002/chem.202101719

DNA[21] and as sensors in enantioselective reactions.[22] Recently, their photophysical properties were investigated in detail.[23]

A second structurally related class of PAHs are dibenzoperylenes (DBPs, Figure 1) with their 26 π-electron system, also known as peropyrenes.[24] Peropyrenes can be formally described as C–H analogues of DDPs and are currently investigated as singlet fission material.[25] It was stated that "a good method to introduce substituents onto peropyrene is still lacking".[26a] Only few examples of modified DBPs were known,[26] none of them with substituents exclusively in 1-, 3-, 8- and 10-position. Recently we described a novel synthetic approach to DDPs and DBPs.[17,27] Our method comprises a reductive functionalization at the carbonyl positions of one of the most prominent organic dyes in photo chemistry and physics, perylenetetracarboxylic diimide (PTCDI) and the introduction of four replaceable and versatile triflate substituents. We also demonstrated a reductive silylation and functionalization approach of peropyrenes higher homologues terropyrene and quarterropyrene.[28] Independently, Miyake et al. reported a reductive transformation of naphthalene tetracarboximide (NTCDI) and PTCDI to tetrapivaloyl substituted 2,7-diazapyrenes and DDPs utilizing zinc or manganese as reducing agents.[29–31] Two examples of Ni-catalyzed Suzuki-Miyaura cross-coupling reactions of such 2,9-diazaperopyrene-tetrapivaloates with a fourfold molar excess of two aryl boronic acids toward 2,9-diaza-1,3,8,10-tetra(4-tert-butylphenyl)-peropyrene (65% yield) and -tetra(5-methylthienyl)-peropyrene (10% yield) were reported.[31]

Results and Discussion

Syntheses and characterization of DDP and DBP

Independently from Miyakes tetrapivaloyl route[31] we developed a protocol for reductive silylation and conversion of PTCDI into 1,3,8,10-tetratriflato-2,9-diazaperopyrene **3a** (Scheme 2).[17] Details are presented here. Triflate groups in key intermediate **3a** tend to be more reactive and more versatile in their reaction patterns than pivaloate groups. They turned out to undergo not only Suzuki-Miyaura coupling with a larger set of aryl boronic acids and without need of using the latter in large molar excess. Furthermore, triflates are able to undergo Sonogashira cross-coupling reactions or direct uncatalyzed nucleophilic substitution reactions. And they could be installed not only in 1,3,8,10-tetratriflato-2,9-diazaperopyrene **3a** but also in corresponding dimethyl-peropyrene **3b** (Scheme 2).

Scheme 1 displays the first reductive functionalization step towards soluble tetrasiloxy-2,9-diazaperopyrene **2a** and 2,9-dimethyl-dibenzoperylene **2b**. PTCDI (**1a**) is reduced using sodium in diglyme at 160 °C at a 70-gram scale. The precipitating sodium salt of reduced PTCDI is reacted in situ with trimethylsilyl chloride forming highly soluble **2a** in good yields of around 55%. Another synthetic route towards **2a** was reported using *n*-butyllithium as reducing agent for PTCDI.[16a]

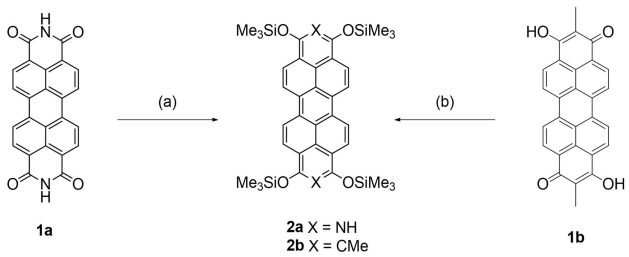

Scheme 1. Synthesis of **2a** and **2b**: (a) 1. Na (4.4 equiv), diglyme, 160 °C, 6 h; 2. TMSCl (6.0 equiv), rt, 3 d, then 160 °C, 3 h, 55%; (b) 1. C_8K (4.3 equiv), THF, 55 °C, 3 d, then 65 °C, 8 h; 2. TMSCl (6.0 equiv), 60 °C, 8 h, 22%.

Peropyrene **2b** was obtained via reduction of dihydroxy peropyrenequinone **1b** using potassium graphite (C_8K) as reducing agent and trimethylsilyl chloride (TMSCl) as trapping reagent. Overall, sodium in diglyme seems to be the preferred reducing agent due to its easy handling on a multigram scale. Starting material **1b** was synthesized via an oxidative coupling of 2-methyl 3-hydroxy-1-phenalenone in a potassium hydroxide melt[17] modifying similar oxidative reactions.[27,33] This oxidative coupling followed by reductive triflylation protocol allowed the introduction of other organic groups in 2,9- and 1,3,8,10-position of peropyrenes.[27]

Orange solid **2a** can be handled under aerobic atmosphere, however in solution and in presence of air and moisture, **2a** is re-oxidized to starting material PTCDI, which is deposited as thin film on the inner glass surface of the flask, as is verified by IR spectroscopy (Figure S1). This selective aerobic reoxidation and deposition reaction can be used to fabricate pure and transparent PTCDI films from solution.

In the second step, **2a** is activated and trimethylsilyl groups are replaced by triflyl groups. We obtained key intermediate **3a** in 60% yield upon treating **2a** with trifluoromethanesulfonic anhydride (Tf_2O) in the presence of equimolar amounts of *N*,*N*-dimethyl-4-aminopyridine (DMAP) as activating agent for Tf_2O (Scheme 2). *N*-Methylimidazole may also be used as a Tf_2O activating agent. A second method yielded **3a** in 34% yield via reaction of Tf_2O with tetralithium salt **8** generated by desilylation of **2a** with *n*-butyllithium (*n*-

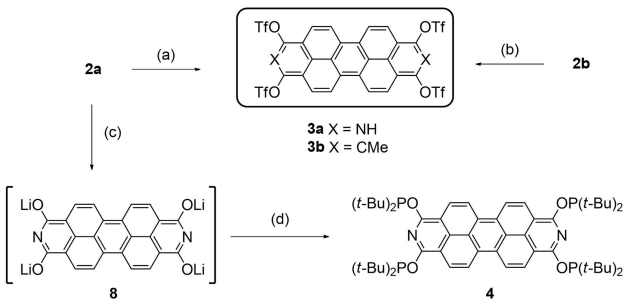

Scheme 2. Synthesis of **3a**, **3b** and **4**: (a) DMAP (4.0 equiv), Tf_2O (4 equiv), CH_2Cl_2, rt, 22 h, 60%; (b) 1. *n*-BuLi (4.0 equiv), 2. Tf_2O (4.0 equiv), 0 °C, 16 h, Et_2O, 54%); (c) *n*-BuLi (4.0 equiv), Et_2O, rt, 3 d, (quant.); (d) *t*-Bu_2PCl (8.0 equiv), DMF, 80 °C, 4 d, 82%.

BuLi). This method turned out to be the better one when **2b** was desilylated by four equivalents of *n*-BuLi. Treatment of in situ forming and precipitating tetralithium salt with Tf_2O in diethyl ether yielded tetratriflate DBP **3b** in 54% yield. Careful handling of **3b** is required since it decomposes rapidly in air at ambient light. The synthetic viability of PTCDI derived tetralithium salt **8** in reactions with electrophiles is demonstrated by its use as synthon in the high-yield synthesis of tetraphosphinate **4**, a potential bifunctional PONOP pincer ligand in 82% yield (Scheme 2).

Tetratriflates **3a** and **3b** are versatile key intermediates in the synthesis of highly functionalized DDPs and DBPs. In this report we focus on the synthesis of DDPs, the functionalized DBP series is reported separately.[27] Three representative examples of functionalization reactions for DDP **3a** are shown in Scheme 3. Firstly, Suzuki-Miyaura cross-coupling reactions were carried out using phenyl boronic acids (1.5 instead of 4.0 eq per functional group) and catalytic amounts of $Pd(PPh_3)_4$ (2.5 mol% per functional group) to obtain 1,3,8,10-tetraaryl DDPs **5a**–**5e**. The yield for **5b** is similar to previously reported applying tetrapivaloates with fourfold excess of boronic acid per functionality.[31] DDP **5a** is a red soluble C_{48}–PAH, sublimable at temperatures $>350\,^{\circ}C$ and 10^{-3} mbar. Noteworthy, we were able to provide a chromatography-free work-up of **5a**–**5d**. Secondly, a representative Sonogashira reaction was carried out with trimethylsilylacetylene and catalytic amounts of $PdCl_2(Po\text{–}Tol_3)_2$ (0.17 equiv) to produce **6** in 15% yield, a transformation not accessible via tetrapivaloates so far. Stoichiometric amounts of $[n\text{-}Bu_4N]I$ were added to the reaction in order to in situ substitute OTf moieties with iodine groups and for providing a superior reactivity compared to triflate in some cross coupling reactions. Desilylation of tetraethinyl derivative **6** will allow further modifications such as Glaser couplings or other cross-coupling, cycloaddition, or ring annulation reactions. Finally, we made use of the accessibility of triflate groups in **3a** for uncatalyzed nucleophilic substitution reactions, again a strategy not available for less reactive tetrapivaloates. In this respect, **3a** was used in direct nucleophilic amination with piperidine to obtain **7**. The substitution proceeds nearly instantaneously as observed by a color change to a purple solution. Air-sensitive, very electron-rich tetra-piperidyl derivative **7** was obtained in pure form by simply washing the crude solid with degassed water.

We obtained single crystals suitable for low-temperature X-ray crystallographic analysis of **2a**, **2b**, **3a**, **4**, **5b** and **5c**. Their molecular and lattice structures are presented in Figure 2 and Figure S7. All compounds adopt a highly planar central DPP conformation with only little deviation of atoms from the mean aromatic plane: av. 0.04 Å, 0.02 Å, 0.03 Å and 0.05 Å for **2b**, **3a**, **4** and **5c**, respectively. **2a** and **5c** crystallize in triclinic space group *P*-1 with a slip stacked arrangement and with shortest inter-plane arene contacts of 3.39 Å and 3.49 Å, therefore exhibiting significant π-π interactions. **2b**, **3b** and **5b** crystallize in monoclinic space groups $P2_{1/n}$, $P2_1$ and $P2_{1/n}$ in a heringbone-like arrangement with similarly short distances of the aromatic planes (3.56 Å and 3.38 Å for **2b** and **3b**). **5b** forms dimers with intra-dimer distances of 3.62 Å und inter-dimer distances of 3.78 Å, indicating a weaker interaction than that of **5c. 4** crystallizes in the orthorhombic space group

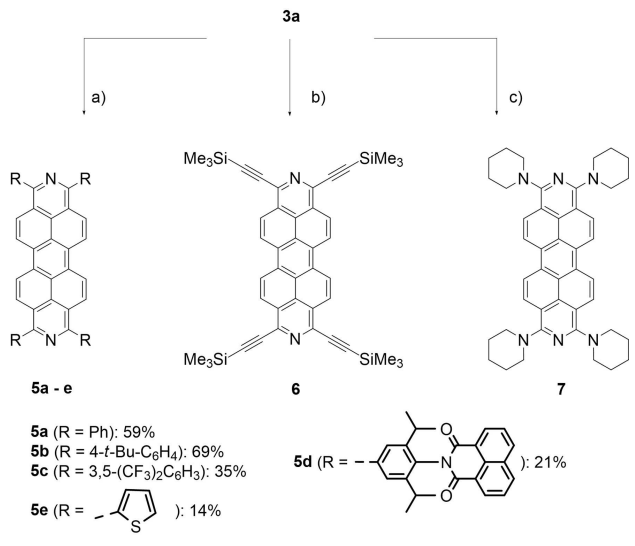

Scheme 3. Functionalization reactions of triflate **3a**: (a) $R\text{–}B(OH)_2$ (6.0 equiv), $Pd(PPh_3)_4$ (0.1 equiv), $NaHCO_3$ (aq), Tol/EtOH, 90 °C, 12 h–7 d; (b) trimethylsilylacetylene (6.0 equiv), $PdCl_2(Po\text{–}Tol_3)_2$ (0.2 equiv), CuI (0.6 equiv), Bu_4NI (6.0 equiv), DMF/Et_3N, rt, 3 h, 15%. (c) piperidine (17 equiv), DMSO, 90 °C, 20 h, 63%.

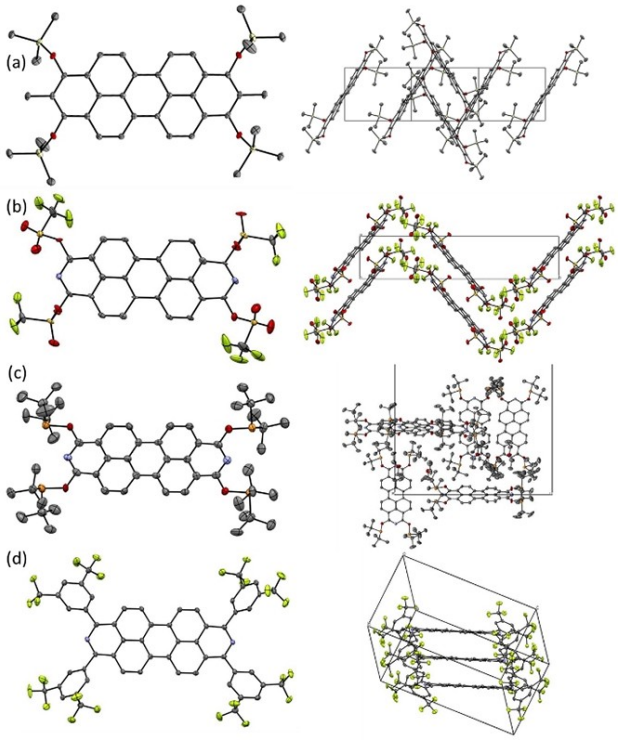

Figure 2. Molecular and packing structures of (a) **2b**, (b) **3a**, (c) **4** and (d) **5c**. Hydrogen atoms and solvents molecules are omitted for clarity. Thermal ellipsoids are shown at 50% probability.

$P2_12_12$ and exhibits no π-stacking due to four sterically demanding –OP*t*-Bu_2 groups.

All molecules reveal very similar C–C bond lengths of the DPP core ranging from 1.350(3) Å to 1.433(4) Å. On the basis of the C–C-bond lengths between naphthalene subunits (C–C 1.47 Å, Figure S8), parent PTCDI is well described as two fused naphthalene units.[32] Contrastingly, the investigated DDPs have shorter C–C-bond lengths between the naphthalene subunits (1.42 Å). According to the bond length pattern, the aromaticity of the DDPs and DBP **3b** can be described according to Clar's sextett model with the three axially located central benzene rings as Clar sextetts (see Figure S8).[35–36]

Figure 4 displays the UV/Vis and emission spectra of selected compounds in CH_2Cl_2. The influence of the 2,9-position (nitrogen versus carbon atom) is investigated for DDPs **2a** and **3a** and DBPs **2b** and **3b**. Dyes **2** and **3** show pronounced vibronic progression fine structures with spacings of ~30 nm in the absorption and mirrored emission spectra typical for diazadibenzoperylenes and dibenzoperylenes.[25] The emission maxima are bathochromically shifted for **2a** and **3a** compared to **2b** and **3b**. The redshifted emission maxima and the larger Stokes shifts for DDPs (Table 1) indicate a more pronounced configurational change between the ground state and the excited state and higher reorganization energy loss between absorption and emission, possibly caused by the nitrogen-induced dipole momentum change upon excitation.

The introduction of electron-rich substituents in 1,3,8,10-position leads to an increased bathochromic shift of the absorption and emission maxima. The absorption maxima range from 455 nm for the electron-poor tetratriflate **3a** to 550 nm for the most electron-rich tetrapiperidino substituted **7**. Emission maxima range from 473 nm (**3a**) to 583 nm (**7**). Both, absorption and emission spectra demonstrate the optical tunability of DDPs by functionalization of positions *ortho* to the nitrogen atoms. The vibronic fine structure is less pronounced for **4**, **5** and **7**. Contrastingly, **6** exhibits a pronounced vibronic fine structure and a small Stokes shift of 7 nm (253 cm^{-1}) indicating a more rigid aromatic backbone.

Table 1. Summary of photophysical data.[a]

Compound	$\lambda_{abs,max}$ [nm]	$\lambda_{em,max}$ [nm][b]	Stokes shift [cm^{-1}]	$E_{g,opt}$ [eV][d]
2a	490	508	723	2.48
2b	479	488	385	2.57
3a	455	474	881	2.68
3b	457	466	423	2.68
4	498	540	1562	2.44
5a	490	517	1066	2.45
5a[c]	487	551	2385	2.36
5b	497	528	1181	2.41
5c	490	521	1214	2.45
5d	502	538	1333	2.37
5e	543	574	995	2.21
5e[c]	519	612	2928	2.15
6	522	529	253	2.36
7	550	583	1029	2.19

[a] Solvent, CH_2Cl_2; [b] excitation wavelength 350 nm; [c] 5 vol-% TFA added; [d] determined from the intersection wavelength of normalized absorption and emission spectra.

The addition of 5 vol-% trifluoroacetic acid (TFA) to a CH_2Cl_2 solution of **5a** and **5e** causes their protonation and a bathochromic shift of the emission (Figure S2, S3 and S4).

The electrochemical properties of structurally related **5a**–**5e** were investigated by cyclovoltammetry and differential pulse voltammetry (Table 2, Figures 3 and S5). **5a** exhibits two reversible reduction and oxidation waves, which are lower for **5c** and **5d** with more electron-withdrawing substituents. Compared to more electron-rich **5b** and **5e** the opposite trend is observed for the oxidation waves, indicating a strong influence of the 1,3,8,10-subsituents on the LUMO energies of these DDP derivatives, in particular. Overall, the obtained experimental and calculated HOMO and LUMO energies (Table 2, Figure 5, Table S1) are in good agreement for **5a**, **5b** and **5e** and confirm the trend for **5c**.

DFT calculations

The trends of absorption maxima (Figure 4) is supported by TD-DFT calculations at PBE0-D3(BJ)/def2-TZVPP level of theory (see Table S2-S15 for details). In all cases, the lowest-energy absorption band is correlated to a HOMO-LUMO (S_0 to S_1) electronic transition. Furthermore, the influence of electron-withdrawing and electron-releasing substituents on the photo-

Table 2. Redox Potentials of **5a**–**5e** vs. Fc/Fc^+.

	E_{red2} [V]	E_{red1} [V]	E_{ox1} [V]	E_{ox2} [V]	$E_{HOMO,exp}$ [eV][a]	$E_{LUMO,exp}$ [eV][b]
5a	−2.29	−1.96	0.51	1.02	−5.31	−2.86
5b	−2.32	−1.97	0.36	0.64	−5.16	−2.75
5c	−1.93	−1.71	0.76	1.12	−5.56	−3.11
5d	−2.17	−1.91	0.71	1.27	−5.51	−3.14
5e	−2.01	−1.75	0.39	0.66	−5.19	−2.98

[a] Redox potentials of **5a**–**5e** (measured in CH_2Cl_2, 0.1 M *n*-Bu_4NPF_6) vs. Fc/Fc^+. [b] Determined using literature methods by referencing on Fc/Fc^+ as internal standard (E_{HOMO} (Fc) = −4.8 eV): $E_{HOMO,exp}$ = −4.8 eV–E_{Ox1}.

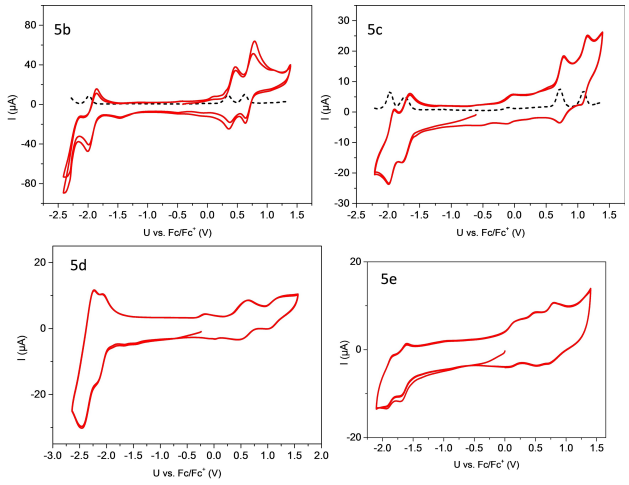

Figure 3. Cyclic voltammetry (solid line) and differential pulse voltammetry (dashed line) of **5b**–**5e**. Measurements were performed in a saturated CH_2Cl_2 solution with 100 mM *n*-Bu_4NPF_6 as electrolyte.

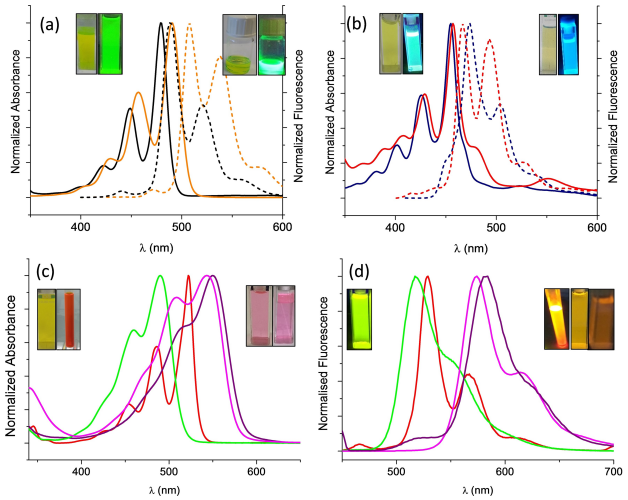

Figure 4. (a) UV/Vis absorption (line) and emission (dashed) spectra of **2a** (orange) and **2b** (black); (b) UV/Vis absorption (line) and emission (dashed) spectra of **3a** (navy) and **3b** (red); (c) UV/Vis absorption spectra and (d) emission spectra of **5a**, **5e**, **6**, **7** (green, magenta, red, and purple line). All samples were measured in CH_2Cl_2. Inset: Photo images of the respective samples ($c \approx 10^{-5}$ M) under ambient light and under excitation at 366 nm.

physical and electroanalytical properties of **2**–**3** and **5**–**7** was rationalized. Molecular orbital diagrams are shown in Figure 5 and Figure S9.

The frontier Kohn-Sham orbitals and energies support our experimental observation that substituents in 1,3,8,10-position strongly influence the electronic properties. Both, HOMO and LUMO are delocalized over the DDP backbone and to some extent over the *ortho* substituents, as shown in Figure 5. This participation of the substituents to the frontier orbitals explains a strong effect on the optoelectronic properties of DDPs. The participation of the substituents to the frontier orbitals is especially pronounced for **2**, **3**, **5e**, **6** and **7**. The substituents in **6** are contributing via the conjugated triple bond π system, while in **2**, **3** and **7** the oxygen and nitrogen atoms are directly contributing to the HOMO and LUMO coefficients of the aromatic system. As expected, electron-withdrawing substituents such as triflate (**3a**) or 3,5-bis (trifluormethyl)phenyl (**5c**) lead to low-lying frontier orbitals, whereas electron-donating substituents such as 2-thienyl (**5e**) and piperidinyl (**7**) lead to energetically high-lying frontier orbitals. However, as observed for highly reactive triflates **3a**,**b**, energetically low-lying HOMO and LUMO frontier orbitals do not guarantee any air stability as an energetically low-lying LUMO may be attacked by water as nucleophile while a high-lying HOMO is giving rise to oxygen sensitivity.

The influence of [N] versus [CMe] building blocks in 2,9 positions on the HOMO and LUMO energies (Table S1 and Figure S9) is calculated for the new title compounds and triflate key intermediates **3a** and **3b**. As expected sp^2 nitrogen atoms in the 2,9-position lead to a stabilization of the frontier orbitals. The same trend was reported for similar tetrasubstituted peropyrenes[27] and related 2,8-diazaperylenes, recently.[37]

Conclusions

The strategy of reductive O-silylation and O-trifylation of PTCDI, one of the most prominent industrially produced dyes, and its transformation into highly versatile and reactive 1,3,8,10-tetratriflato-2,9-diazadibenzoperylene (**3a**) at multi-gram scale was presented in detail. A similar protocol was available for corresponding 1,3,8,10-tetratriflato-2,9-dimethyldibenzoperylene (**3b**). Key compound **3a** was further applied in Pd-catalyzed cross-coupling reactions towards representative tetra-aryl, -heteroaryl and -alkynyl 2,9-diazaperopyrenes **5a**–**e** and **6**. Without need for any catalyst, reactive triflato groups could be replaced by secondary amino groups such as 1-piperidinyl in **7**, whereas O–$SiMe_3$ groups in **2a** could be replaced by O-phosphanyl (O-P*t*-Bu_2) groups in **4**. The molecular and lattice structures of **2a**, **2b**, **3a**, **4**, **5b**, and **5c** reveal essentially planar DDP and DBP cores. Due to four sterically bulky substituents the intermolecular aggregation is rather weak and led to moderate to high solubility. The

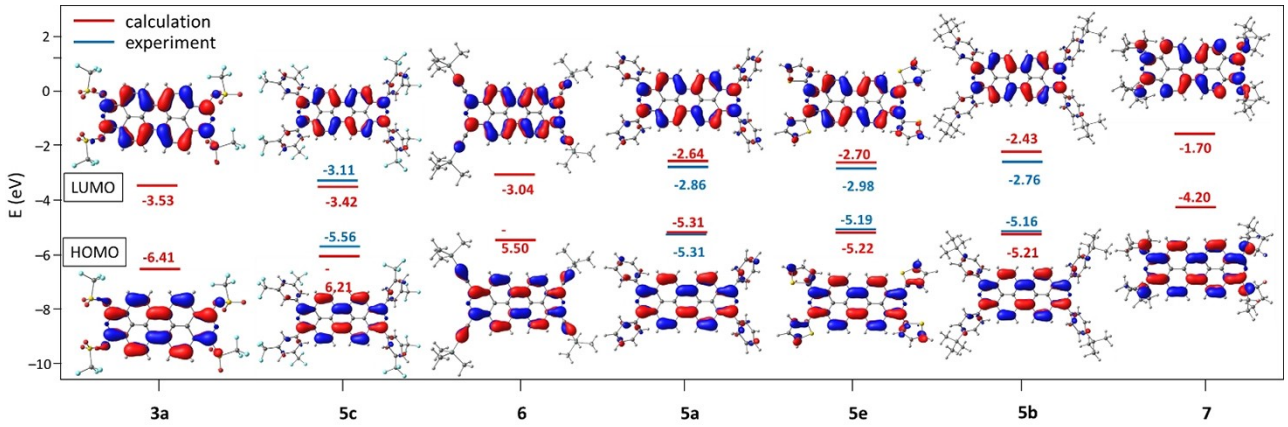

Figure 5. Calculated and experimentally determined molecular orbital energies and Kohn-Sham-orbitals of HOMO and LUMO for **3a**, **5a**–**5c**, **5e**, **6** and **7**. The corresponding Kohn-Sham orbitals of HOMO and LUMO are shown as insets (isoval. 0.03 a.u.).

representative set of electron-withdrawing and -donating substituents at 1,3,8,10-positions have an impact on the absolute HOMO and LUMO levels and on the HOMO-LUMO gap, as rationalized via UV/Vis and PL spectroscopy, by CV and correlated with results of DFT and TD-DFT calculations. Absorption maxima ranging from 455 nm to 550 nm and emission maxima from 474 nm to 583 nm were correlated with the electronic nature of the substituents. Our approach will allow to develop the chemistry of prominent electron-poor dye PTCDI into more electron-rich optoelectronic, organic semiconductors and fluorescent materials.

Experimental Section

Methods and materials: All reactions were carried out under inert nitrogen atmosphere using Schlenk techniques if not mentioned otherwise. All reagents were purchased from commercial sources if not mentioned otherwise and were used without further purification. All solvents were dried and/or purified according to standard procedures and stored over 3 Å or 4 Å molecular sieves.

NMR spectra were recorded in automation or by the service department of Fachbereich Chemie, Philipps Universität Marburg with a Bruker Avance 300, 400, or 500 spectrometer at 300 K using d_1-TFA, CD_2Cl_2 or $CDCl_3$ as solvent and for calibration. If not stated otherwise, heteronuclear NMR spectra were recorded proton decoupled.

The data collection for the single-crystal structure determinations of **2b**, **3a**, and **5c** was performed with a BRUKER D8 QUEST diffractometer at low temperature (100 K) by the X-ray service department of the faculty of chemistry, University of Marburg. The device is equipped with a Mo–K_α X-ray micro source, a fixed chi goniometer and a PHOTON 100 CMOS detector. BRUKER software (APEX2, SAINT) was used for data collection, cell refinement and data reduction.[38] The data collection for the single-crystal structure determinations of **2a**, **4**, **5b** was performed with a STOE STADIVARI diffractometer at low temperature (100 K) by the X-ray service department of the faculty of chemistry, University of Marburg. The device is equipped with a Cu-K_α X-ray micro source, a four circle goniometer and a DECTRIS PILATUS 300 K detector. The STOE X-Area software package was used for data collection, cell refinement and data reduction.[38] The structures were solved with SHELXT-2014[39] refined with SHELXL-2014[40] and finally validated using PLATON[41] software, all within the WinGX[42] software bundle. Absorption corrections were applied first within the APEX2 or X-Area software (multi-scan).[38] Graphic representations were created using Mercury 3.10.3. The C-bound H-atoms were constrained to parent site. The ellipsoids are shown with 50% probability level in all graphics and the hydrogen atoms are displayed with arbitrary radii.

Deposition Numbers 2080319 (for **2a**), 2077952 (for **2b**), 2080320 (for **3a**), 2080321 (for **4**), 2077954 (for **5b**), and 2080322 (for **5c**) contain the supplementary crystallographic data for this paper. These data are provided free of charge by the joint Cambridge Crystallographic Data Centre and Fachinformationszentrum Karlsruhe Access Structures service www.ccdc.cam.ac.uk/structures.

Note: a room temperature data collection and results of a single-crystal structure XRD analysis of **5b** has been deposited under CCDC 1912582 previously.

HR-APCI mass spectra were acquired with a LTQ-FT Ultra mass spectrometer (Thermo Fischer Scientific). The resolution was set to 100.000. HR-FD mass spectra were acquired with a AccuTOF GCv 4G (JEOL) Time of Flight (TOF) mass spectrometer. An internal or external standard was used for drift time correction. The LIFDI ion source and FD-emitters were purchased from Linden ChroMasSpec GmbH (Bremen, Germany).

All IR spectra are recorded with a Bruker Alpha FTIR spectrometer with Platinum ATR sampling in a glovebox. Absorption spectra were recorded with a Varian Cary-5000 UV/Vis/NIR spectrophotometer in 10 mm cuvettes in CH_2Cl_2 with concentrations of 10 μM to 30 μM with a scan rate of 600 nm/min. Emission spectra were recorded with a Varian Cary Eclipse Spectrophotometer in 10 mm cuvettes in CH_2Cl_2 with a scan rate of 600 nm/min.

Cyclic voltammetry and differential pulse voltammetry measurements are carried out on a rhd instruments TSC 1600 closed electrochemical workstation (working electrode: glassy carbon; counter electrode: platinum crucible; reference electrode: platinum wire (pseudo reference electrode under nitrogen atmosphere in a glovebox (Labmaster 130, MBraun). The samples were measured in CH_2Cl_2 and calibrated using ferrocene as internal standard after measurements. CH_2Cl_2 was purified according to literature and filtered through an aluminum oxide pad prior to use. Tetrabutylammonium hexafluorophosphate ($TBAPF_6$; ≥99.0%) is used as electrolyte for electrochemical analysis. The measurements were carried out at a concentration of 100 mmol/L of electrolyte and 5 mM sample.

Selected synthetic procedures: A detailed description of all preparative procedures and characterization of compounds is deposited in the Supporting Information.

Dihydroxyperopyrenequinone (1b):[17,33] Naphthalic anhydride (10.0 g, 50.5 mmol, 1.0 equiv), diethyl methylmalonate (26.0 g, 151.4 mmol, 3.0 equiv) and $ZnCl_2$ (15.1 g, 111.0 mmol, 2.2 equiv) were stirred for 15 min at 25 °C and 5 h at 195 °C. The solidified orange product mixture was dissolved in NH_3 (5% in H_2O) and filtered. The red filtrate was acidified with hydrochloric acid, the yellow precipitate was filtered off and washed with H_2O. Recrystallization from toluene yielded the product (7.75 g, 36.9 mmol, 73%) as yellow needles. ^{1}H NMR (300 MHz, $CDCl_3$): δ = 8.43 (d, J = 6.5 Hz, 2H), 8.09 (dd, J = 8.0, 7.0 Hz, 2H), 7.68 (dd, J = 8.0, 7.0 Hz, 2H), 2.19 (s, 3H) ppm. ^{13}C NMR (75 MHz, $CDCl_3$): δ = 133.1, 131.9, 126.6, 113.1, 7.9 ppm. APCI-HRMS(−) ($C_{14}H_9O_2$): found (calc.) m/z = 209.0608 (209.0608). This intermediate product, 3-hydroxy-2-methyl-1-phenalenone (7.5 g, 35.7 mmol) was mixed with KOH (25 g) and heated to 270 °C for 2 h. The black mixture was dissolved in 600 mL H_2O and filtered. The violet filtrate was acidified with hydrochloric acid and the brown precipitate filtered off. The product was suspended in hot methanol and washed until the filtrate was colorless. The product was obtained as black solid (7.0 g, 16.8 mmol, 94%). APCI-HRMS(−) ($C_{28}H_{15}O_4$): found (calc.) m/z = 417.1121 (417.1123).

2,9-Diaza-1,3,8,10-tetrakis(trimethylsilyloxy)dibenzoperylene (2a): PTCDI (71.3 g, 182.7 mmol, 1.0 equiv) and sodium (18.4 g, 0.8 mmol, 4.4 equiv) were stirred in 400 mL diglyme for 6 h at 160 °C. Trimethylsilyl chloride (140 mL, 6 equiv) was added in portions and the suspension stirred 4 d at room temperature and 3 h at 160 °C. All volatile compounds were removed *in vacuo*, the product was dissolved in CH_2Cl_2 (ca. 300 mL) and the solution was filtered. The solvent was removed *in vacuo* and the product was obtained via crystallization from toluene (68.6 g, 100.8 mmol, 55%). ^{1}H NMR (300 MHz, $CDCl_3$): δ = 8.65 (d, J = 9.5 Hz, 4H), 8.28 (d, J = 9.5 Hz, 4H), 0.57 (s, 36H) ppm. ^{13}C NMR (75 MHz, $CDCl_3$): δ = 154.6, 134.4, 126.4, 124.3, 122.5 (CH (δ = 8.28 ppm)), 112.0 (CH (δ = 8.65 ppm)), 110.8, 0.9 (CH_3) ppm. FD-HRMS(+) ($C_{36}H_{44}N_2O_4Si_4$): found (calc.) m/z = 680.23605 (680.23781). FTIR: ν = 2955 (m), 2901 (w), 2853 (w), 1624 (m), 1584 (m), 1545 (s), 1485 (m), 1467 (w), 1396 (s),

1360 (m), 1301 (s), 1247 (s), 1177 (m), 1096 (w), 977 (s), 929 (m), 838 (vs), 781 (s), 750 (m), 708 (m), 642 (m), 595 (m), 562 (w), 466 (w) cm^{-1}. Elemental analysis for $C_{36}H_{44}N_2O_4Si_4$ (681.10 g/mol), found (calc.)%: C 63.85 (63.49), N 3.84 (4.11), H 6.70 (6.51). UV/Vis (CH_2Cl_2): λ_{abs} = 490, 457, 429 nm. PL (CH_2Cl_2, λ_{ex} = 350 nm): λ_{em} = 471, 508, 538, 577 nm.

2,9-Dimethyl-1,3,8,10-tetrakis(trimethylsilyloxy)dibenzoperylene (2b): **1b** (2.5 g, 6.0 mmol, 1.0 equiv) and C_8K (3.5 g, 25.9 mmol, 4.3 equiv) were suspended in 100 mL THF and stirred for 3 d at 55 °C and 8 h at 65 °C. Trimethylsilyl chloride (4.5 mL, 36.0 mmol, 6.0 equiv) was added slowly at room temperature and stirred over night at 60 °C. Volatile compounds were removed under reduced pressure, the remaining solid dissolved in CH_2Cl_2 and filtered. The solution was filtered through a pad of silica gel and the product washed with pentane. The pure product was obtained as orange solid (0.92 g, 1.3 mmol, 22 %). ^{1}H NMR (300 MHz, $CDCl_3$): δ = 9.01 (d, J = 9.5 Hz, 4H), 8.42 (d, J = 9.5 Hz, 4H), 2.59 (s, 6H), 0.41 (s, 36H) ppm. ^{13}C NMR (126 MHz, $CDCl_3$): δ = 149.6 ($COSiMe_3$), 125.6, 125.1, 123.7, 121.9 (CH), 120.4 (CH), 119.1, 13.2 (CH_3), 1.2 ($SiMe_3$) ppm. ^{29}Si NMR (99 MHz, $CDCl_3$): δ = 22.4 ppm. FD-HRMS(+) ($C_{40}H_{50}O_4Si_4$): found (calc.) m/z = 706.27735 (706.27861). FTIR: ν = 2955 (w), 2900 (w), 1626 (w), 1587 (w), 1483 (m), 1405 (m), 1387 (m), 1365 (w), 1343 (w), 1304 (m), 1248 (m), 1221 (m), 1172 (m), 1145 (m), 1101 (m), 1034 (w), 915 (s), 838 (s), 787 (m), 756 (m), 705 (m), 691 (m), 657 (m), 568 (w), 457 (w) cm^{-1}. Elemental analysis for $C_{36}H_{44}N_2O_4Si_4$ (707.16 g/mol), found (calc.)%: C 64.39 (67.94), H 6.77 (7.31).

2,9-Diaza-1,3,8,10-tetratriflato-dibenzoperylene (3a)

Method A: **2a** (8.00 g, 11.7 mmol, 1.0 equiv) was dissolved in Et_2O (250 mL) and slowly treated with *n*-BuLi (2.75 M in hexane, 17.1 mL, 47.0 mmol, 4.0 equiv) at room temperature. Tf_2O (7.90 mL, 13.2 g, 47.0 mmol, 4.00 equiv) was slowly added after 18 h at −78 °C (1.75 mL/h) and stirred for 1 d. The suspension was filtered and washed with THF. The remaining solid was extracted with hot chloroform and the product obtained after the removal of the solvent under reduced pressure as orange powder (3.66 g, 0.4 mmol, 34 %). ^{1}H NMR (300 MHz, $CDCl_3$): δ = 9.50 (d, J = 9.0 Hz, 4H), 8.70 (d, J = 9.0 Hz, 4H) ppm. ^{13}C NMR was not collected due to low solubility. ^{19}F NMR (282 MHz, $CDCl_3$: δ = −72.0 ppm. FD-HRMS (+) ($C_{28}H_8F_{12}N_2O_{12}Si_4$): found (calc.) m/z = 919.87528 (919.87684). Elemental analysis for $C_{28}H_8F_{12}N_2O_{12}S_4$ (920.60 g/mol), found (calc.)%: C 37.08 (36.53), N 3.10 (3.04), H 1.21 (1.18), S 13.99 (13.93). FTIR: ν = 1411 (m), 1349 (m), 1214 (s), 1168 (m), 1122 (s), 1029 (m), 947 (m), 907 (m), 831 (m), 788 (s), 751 (m), 637 (m), 597 (s), 495 (s) cm^{-1}. UV/Vis (CH_2Cl_2): ε (λ_{abs}) = 56800 (455 nm), 33600 (426 nm), 17500 (402 nm), 9000 (381 nm) $L \cdot mol^{-1} \cdot cm^{-1}$. PL ($CH_2Cl_2$, 19.15 μM, λ_{ex} = 400 nm): λ_{em} = 474, 502, 540 nm. **3a** decomposes with an excess of Tf_2O within hours. Therefore, very slow addition of Tf_2O to tetralithium salt **8** is essential.

Method B: **2a** (0.46 g, 0.64 mmol, 1.0 equiv) and 4-dimethylaminopyridine (DMAP) (0.03 g, 0.3 mmol, 4.0 equiv) were suspended in 30 mL CH_2Cl_2 and Tf_2O (0.45 mL, 2.56 mmol, 4.0 equiv) was added to the orange suspension at room temperature. After 22 h the green solution was evaporated at reduced pressure and the obtained green solid washed with 50 mL pentane. The product (0.38 g, 0.41 mmol, 64 %) was dissolved in CH_2Cl_2 and filtered. The green CH_2Cl_2 solution turned orange upon contact with air, with no change of the NMR spectroscopic properties observed. NMR spectra of the product are identical to the product obtained by Method B. Crystals for structure determination were obtained from a saturated CH_2Cl_2 solution.

2,9-Dimethyl-1,3,8,10-tetratriflato-dibenzoperylene **3b**: To **2b** (0.05 g, 0.07 mmol, 1 equiv) in 50 mL Et_2O was slowly added *n*-BuLi (2.5 M in hexane, 0.1 mL, 0.28 mmol, 4 equiv) at 0 °C. A red solid formed and was slowly treated with Tf_2O (0.04 mL, 0.2 mmol, 4.0 equiv) at 0 °C. After 16 h volatile compounds were removed under reduced pressure and the solid dissolved in 20 mL CH_2Cl_2. The green suspension was filtered through a pad of dry silica gel to obtain a yellow solution of the product. The solvent was removed *in vacuo* and **3b** obtained as yellow solid (0.03 g, 0.04 mmol, 54 %). ^{1}H NMR (300 MHz, $CDCl_3$: δ = 9.22 (d, J = 9.5 Hz, 4H), 8.52 (d, J = 9.5 Hz, 4H), 2.91 (s, 6H) ppm. ^{13}C NMR was not collected due to low solubility ^{19}F NMR (282 MHz, CD_2Cl_2): δ = −72.8 (s) ppm. FD-HRMS (+) ($C_{32}H_{14}F_{12}O_{12}S_4$): found (calc.) m/z = 945.91692 (945.91765).

2,9-Diaza-1,3,8,10-tetra-(di-*tert*-butylphosphinato)-dibenzoperylene (4): **2a** (10.0 g, 14.7 mmol, 1.0 eq.) was dissolved in 200 mL Et_2O and treated with *n*-BuLi (2.45 M in *n*-hexane, 24.0 mL, 58.7 mmol, 4.0 eq.) at room temperature. After 3 d stirring the red precipitate **8** was filtered, washed with *n*-pentane and dried. **8** (0.61 g, 1.5 mmol, 1.0 equiv) was suspended in 50 mL DMF and di-*tert*-butylchlorophosphine (2.71 g, 11.8 mmol, 8.0 equiv) was added. The reaction mixture was stirred for 4 d at 80 °C. DMF and starting materials were removed *in vacuo* (10^{-3} mbar). The residue was dissolved in chloroform, the solution was filtered, and reduced in volume and the product was precipitated by layering with *n*-pentane. The pure product was obtained as red-brown solid (1.17 g, 1.20 mmol, 82 %). ^{1}H NMR (300 MHz, $CDCl_3$): δ = 8.83 (d, $^3J_{HH}$ = 9.0 Hz, 4H), 8.52 (d, $^3J_{HH}$ = 9.0 Hz, 4H), 1.34 (d, $^3J_{PH}$ = 11.0 Hz, 72H) ppm. ^{13}C NMR (75 MHz, $CDCl_3$): δ = 156.5 (d, $^2J_{PH}$ = 8.0 Hz), 134.6, 126.6, 124.7, 122.2, 120.3, 110.1, 36.1 (d, $^2J_{CP}$ = 30.0 Hz), 28.1 (d, $^3J_{CP}$ = 16.0 Hz) ppm. ^{31}P NMR (101 MHz, $CDCl_3$): δ = 153.5 ppm. APCI-HRMS(+) ($C_{56}H_{80}N_2O_4P_4H$): found (calc.) m/z = 969.5142 (969.5141). IR ν = 2938 (m), 2890 (m), 2857 (m), 1685 (s), 1620 (m), 1585 (m), 1545 (m), 1466 (m), 1393 (m), 1349 (m), 1290 (m), 1259 (m), 1197 (s), 1183 (s), 1162 (m), 1084 (m), 1034 (s), 1010 (s), 955 (m), 918 (m), 806 (m), 790 (m), 753 (m), 715 (m), 706 (m), 667 (s), 639 (m), 608 (m), 591 (m), 501 (s), 458 (m), 427 (m) cm^{-1}. UV/Vis (CH_2Cl_2): λ_{abs} = 498, 462, 434 nm. PL (CH_2Cl_2, λ_{ex} = 450 nm): λ_{em} = 540, 580 nm. CV (CH_2Cl_2, vs. Fc/Fc+): E_{red1} = −0.32 V, E_{ox1} = 0.14 V, E_{ox2} = 0.17 V, E_{ox3} = 0.75 V. Crystals for structure determination were obtained from diethyl ether.

2,9-Diaza-1,3,8,10-tetrakis(3,5-bistrifluoromethylphenyl)-dibenzoperylene (5c): **3a** (0.32 g, 0.35 mmol, 1.0 equiv) and $Pd(PPh_3)_4$ (0.05 g, 0.04 mmol, 0.15 equiv) were suspended in 8 mL toluene. 3,5-Bis(trifluormethyl)phenylboronic acid (0.54 g, 2.1 mmol, 6.0 equiv) was dissolved in 4 mL ethanol and added with 2 mL degassed, saturated aqueous $NaHCO_3$ solution to the reaction mixture and stirred at 90 °C. After 12 h the reaction mixture was filtered through a pad of silica gel, solvent was stripped at reduced pressure and the residue was crystallized from CH_2Cl_2/pentane and washed with *n*-pentane. **5c** was obtained as red solid (0.14 g, 0.12 mmol, 35 %). ^{1}H NMR (300 MHz, $CDCl_3$): δ = 9.47 (d, $^3J_{HH}$ = 9.5 Hz, 4H), 8.62 (d, $^3J_{HH}$ = 9.5 Hz, 4H), 8.49 (s, 8H), 8.14 (s, 4H) ppm. ^{1}H NMR (300 MHz, d_1-TFA): δ = 10.07 (d, $^3J_{HH}$ = 9.5 Hz, 4H), 8.92 (d, $^3J_{HH}$ = 9.5 Hz, 4H), 8.61 (s, 8H), 8.51 (s, 4H) ppm. ^{13}C NMR (75 MHz, d_1-TFA): δ = 146.9, 136.8, 136.3, 133.7, 133.3, 133.2, 133.2, 132.2, 131.7, 129.1, 127.7, 126.6 ppm. ^{19}F NMR (282 MHz, $CDCl_3$): δ = −62.6 (s) ppm. FD-HRMS (+) ($C_{56}H_{20}F_{24}N_2^+$): found (calc.): m/z = 1176.1276 (1176.1243). IR ν = 3092 (w), 1581 (w), 1382 (m), 1340 (s), 1316 (w), 1287 (s), 1274 (s), 1265 (s), 1173 (s), 1134 (s), 1115 (vs), 1082 (s), 995 (w), 900 (s), 873 (m), 848 (m), 796 (s), 750 (m), 726 (m), 699 (m), 682 (s), 646 (m), 581 (w), 560 (w), 505 (w), 444 (w), 408 (w) cm^{-1}. UV/Vis (CH_2Cl_2): ε (λ_{abs}) = 100500 (490 nm), 70500 (462 nm) $L \cdot mol^{-1} \cdot cm^{-1}$. PL ($CH_2Cl_2$, λ_{ex} = 350 nm): λ_{em} = 521, 551 nm. CV (CH_2Cl_2, vs. Fc/Fc$^+$): E_{red2} = −1.94 V, E_{red1} = −1.71 V, E_{ox1} = 0.75 V, E_{ox2} = 0.98 V, E_{ox3} = 1.10 V. Crystals for structure determination were obtained from a toluene/*n*-pentane solution.

2,9-Diaza-1,3,8,10-tetrakis(trimethylsilylethinyl)-dibenzoperylene (6): 3a (0.28 g, 0.3 mmol, 1.0 equiv), CuI (35 mg, 0.18 mmol, 0.6 equiv), $Pd(Po\text{-}Tol_3)_2Cl_2$ (35 mg, 0.05 mmol, 0.17 equiv) and *n*-Bu_4NI tetrabutylammonium iodide (0.66 g, 1.8 mmol, 60 equiv) were dissolved in DMF/Et_3N (5 mL/1 mL) and treated with ethynyltrimethylsilane (0.25 mL, 1.8 mmol, 6.0 equiv). After 3 h at room temperature the conversion was complete (TLC) and the reaction mixture was filtered over silica gel and purified via preparative thin layer chromatography (CH_2Cl_2/pentane 1/1). The product was obtained as red solid (0.04 g, 0.06 mmol, 15%). ^1H NMR (300 MHz, CD_2Cl_2: $\delta = 9.30$ (d, $J = 9.0$ Hz, 4H), 8.81 (d, $J = 9.0$ Hz, 4H), 0.48 (s, 36H) ppm). ^{13}C NMR (126 MHz, CD_2Cl_2): $\delta =$ 137.5, 128.2, 127.6, 127.1, 126.3 (CH, 8.9 ppm), 125.9 (CH, 9.4 ppm), 122.5, 102.6, 101.8, 1.3 ppm. ^{29}Si NMR (99 MHz, CD_2Cl_2): $\delta =$ -15.9 ppm. FD-HRMS(+) ($C_{44}H_{44}N_2Si_4$): found (calc.) $m/z = 712.25662$ (712.25815). IR: $\nu = 3359$ (m), 3358 (w), 3195 (w), 2956 (m), 2922 (vs), 2851 (s), 2185 (w), 2160 (w), 2030 (w), 1658 (m), 1632 (s), 1468 (m), 1467 (w), 1422 (w), 1411 (w), 845 (w) cm^{-1}. UV/Vis (CH_2Cl_2): $\lambda_{abs} = 522$, 486, 454, 428 nm. PL (CH_2Cl_2, $\lambda_{ex} = 350$ nm): $\lambda_{em} = 529$, 567 nm. CV (CH_2Cl_2, vs. Fc/Fc^+): $E_{ox1} = 1.06$ V, $E_{ox2} = 1.46$ V.

2,9-Diaza-1,3,8,10-tetra-1-piperidinyl-dibenzoperylene (7): 3a (0.11 g, 0.12 mmol, 1.0 equiv) in 4 mL DMSO was treated with piperidine (0.15 mL, 2 mmol, 16.6 equiv) at room temperature. The brown suspension turned violet upon amine addition and was stirred 1 h at 90 °C. Volatiles were removed *in vacuo* (10^{-3} mbar) and the residue was washed with degassed water (3×10 mL), Et_2O (2 mL) and *n*-pentane (10 ml). After drying (10^{-3} mbar) a dark violet product was obtained in 63% yield (0.05 g, 0.08 mmol). ^1H NMR (300 MHz, $CDCl_3$): $\delta = 7.88$ (br. s, 8H), 3.18 (m, 16H), 1.85 (m, 16H), 1.67 (m, 8H) ppm. FD-HRMS(+) ($C_{44}H_{88}N_6$): found (calc.) $m/z =$ 660.39695 (660.39404). IR: $\nu = 3359$ (s), 3310 (m), 3192 (m), 3002 (m), 2956 (vs), 2920 (s), 2850 (s), 2813 (m), 1658 (s), 1632 (s), 1580 (w), 1529 (w), 1468 (w), 1411 (m), 1376 (m), 1263 (m), 1244 (m), 1190 (m), 1153 (m), 1134 (m), 1096 (m), 1030 (m), 792 (m), 722 (m), 698 (m), 637 (m) cm^{-1}. UV/Vis (CH_2Cl_2): $\lambda_{abs} = 272$, 555 nm. PL (CH_2Cl_2, $\lambda_{ex} = 350$ nm): $\lambda_{em} = 594$, 632 nm.

Supporting Information available: Additional experimental details, NMR spectra, CV measurements, UV/Vis and TD-DFT spectroscopy, cartesian coordinates of calculated structures (XYZ) and XRD data. The CIF files of the presented structures are provided.

Acknowledgements

Funding by the Deutsche Forschungsgemeinschaft through SFB 1083 is gratefully acknowledged. We also gratefully acknowledge the donation of PTCDI by BASF SE. Open access funding enabled and organized by Projekt DEAL.

Conflict of Interest

The authors declare no conflict of interest.

Keywords: diazaperopyrenes · organic dyes · peropyrenes · perylene diimide · reductive aromatization

[1] S. Rajaram, R. Shivanna, S. K. Kandappa, K. S. Narayan, *J. Phys. Chem. Lett.* **2012**, *3*, 2405–2408.
[2] X. Zhan, A. Facchetti, S. Barlow, T. J. Marks, M. A. Ratner, M. R. Wasielewski, S. R. Marder, *Adv. Mater.* **2011**, *23*, 268–284.
[3] J. Li, Q. Zhang, *ACS Appl. Mater. Interfaces* **2015**, *7*, 28049–28062.
[4] J. E. Anthony, *Angew. Chem. Int. Ed.* **2008**, *47*, 452–483; *Angew. Chem.* **2008**, *120*, 460–492.
[5] T. M. Figueira-Duarte, K. Müllen, *Chem. Rev.* **2011**, *111*, 7260–7314.
[6] M. Gsänger, D. Bialas, L. Huang, M. Stolte, F. Würthner, *Adv. Mater.* **2016**, *28*, 3615–3645.
[7] J. Wu, W. Pisula, K. Müllen, *Chem. Rev.* **2007**, *107*, 718–747.
[8] M. Milton, Q. Cheng, Y. Yang, C. Nuckolls, R. H. Sánchez, T. J. Sisto, *Nano Lett.* **2017**, *17*, 7859–7863.
[9] W. Deng, Y. Shen, J. Qian, Y. Cao, H. Yang, *ACS Appl. Mater. Interfaces* **2015**, *7*, 21095–21099.
[10] T. B. Schon, A. J. Tilley, E. L. Kynaston, D. S. Seferos, *ACS Appl. Mater. Interfaces* **2017**, *9*, 15631–15637.
[11] S. C. Martens, U. Zschieschang, H. Wadepohl, H. Klauk, L. H. Gade, *Chem. Eur. J.* **2012**, *18*, 3498–3509.
[12] B. A. R. Günther, S. Höfener, U. Zschieschang, H. Wadepohl, H. Klauk, L. H. Gade, *Chem. Eur. J.* **2019**, *25*, 14669–14678.
[13] M. Stępień, E. Gońka, M. Żyła, N. Sprutta, *Chem. Rev.* **2017**, *117*, 3479–3716.
[14] J. Mei, Y. Diao, A. L. Appleton, L. Fang, Z. Bao, *J. Am. Chem. Soc.* **2013**, *135*, 6724–6746.
[15] F. Würthner, C. R. Saha-Möller, B. Fimmel, S. Ogi, P. Leowanawat, D. Schmidt, *Chem. Rev.* **2016**, *116*, 962–1052.
[16] a) H. Sachdev, EP 2390253 A1 **2011**; b) B. Gunther, R. Braden, H. Holtschmidt, DE2148225 A1 **1973**; c) F. Würthner, A. Sautter, C. Thalacker, *Angew. Chem. Int. Ed.* **2000**, *39*, 1243–1245; *Angew. Chem.* **2000**, *112*, 1298–1301.
[17] J. Sundermeyer, E. Baal, S. Werner, WO **2019**/229134 A1, priority date May 30th **2018**.
[18] A. Slama-Schwok, J. Jazwinski, A. Bere, T. Montenay-Garestier, M. Rougee, C. Helene, J. M. Lehn, *Biochemistry* **1989**, *28*, 3227–3234.
[19] A. V. Aksenov, N. A. Aksenov, A. S. Lyakhovnenko, I. V. Aksenova, *Synthesis* **2009**, *20*, 3439–3442.
[20] a) P. J. Stang, D. H. Cao, S. Saito, A. M. Arif, *J. Am. Chem. Soc.* **1995**, *117*, 6273–6283; b) A. Sautter, D. G. Schmid, G. Jung, F. Würthner, *J. Am. Chem. Soc.* **2001**, *123*, 5424–5430.
[21] K. J. Hartlieb, L. S. Witus, D. P. Ferris, A. N. Basuray, M. M. Algaradah, A. A. Sarjeant, C. L. Stern, M. S. Nassar, Y. Y. Botros, J. F. Stoddart, *ACS Nano* **2015**, *9*, 1461–1470.
[22] F. Biedermann, W. M. Nau, *Angew. Chem. Int. Ed.* **2014**, *53*, 5694–5699; *Angew. Chem.* **2014**, *126*, 5802–5807.
[23] X. Gong, R. M. Young, K. J. Hartlieb, C. Miller, Y. Wu, H. Xiao, P. Li, N. Hafezi, J. Zhou, L. Ma, T. Cheng, W. A. Goddard, O. K. Farha, J. T. Hupp, M. R. Wasielewski, J. F. Stoddart, *J. Am. Chem. Soc.* **2017**, *139*, 4107–4116.
[24] E. Clar, *Ber. Dtsch. Chem. Ges.* **943**, *76*, 458–466.
[25] V. M. Nichols, M. T. Rodriguez, G. B. Piland, F. Tham, V. N. Nesterov, W. J. Youngblood, C. J. Bardeen, *J. Phys. Chem. C* **2013**, *117*, 16802–16810.
[26] a) W. Yang, J. H. S. K. Monteiro, A. de Bettencourt-Dias, V. J. Catalano, W. A. Chalifoux, *Angew. Chem. Int. Ed.* **2016**, *55*, 10427–10430; *Angew. Chem.* **2016**, *128*, 10583–10586; b) W. Yang, G. Longhi, S. Abbate, A. Lucotti, M. Tommasini, C. Villani, V. J. Catalano, A. O. Lykhin, S. A. Varganov, W. A. Chalifoux, *J. Am. Chem. Soc.* **2017**, *139*, 13102–13109; c) K. Uchida, T. Kubo, D. Yamanaka, A. Furube, H. Matsuzaki, R. Nishii, Y. Sakagami, A. Abulikemu, K. Kamada, *Can. J. Chem.* **2017**, *95*, 432–444; d) Y. Yang, L. Yuan, B. Shan, Z. Liu, Q. Miao, *Chem. Eur. J.* **2016**, *22*, 18620–18627.
[27] S. Werner, T. Vollgraff, J. Sundermeyer, *Chem. Eur. J.* **2021**, https://doi.org/10.1002/chem.202101101, in print.
[28] S. Werner, T. Vollgraff, J. Sundermeyer, *Angew. Chem. Int. Ed.* **2021**, *60*, 13631–13635; *Angew. Chem.* **2021**, *133*, 13743–13748.
[29] T. Nakazato, T. Kamatsuka, J. Inoue, T. Sakurai, S. Seki, H. Shinokubo, Y. Miyake, *Chem. Commun.* **2018**, *54*, 5177–5180.
[30] T. Nakazato, H. Shinokubo, Y. Miyake, *Chem. Commun.* **2021**, *57*, 327–330.
[31] Y. Nakamura, T. Nakazato, T. Kamatsuka, H. Shinokubo, Y. Miyake, *Chem. Eur. J.* **2019**, *25*, 10571–10574.
[32] a) A. J. Tilley, C. Guo, M. B. Miltenburg, T. B. Schon, H. Yan, Y. Li, D. S. Seferos, *Adv. Funct. Mater.* **2015**, *25*, 3321–3329; b) A. J. Tilley, R. D. Pensack, T. S. Lee, B. Djukic, G. D. Scholes, D. S. Seferos, *J. Phys. Chem. Chem. Phys.* **2014**, *118*, 9996–10004; c) D. Jänsch, C. Li, L. Chen, M. Wagner, K. Müllen, *Angew. Chem. Int. Ed.* **2015**, *54*, 2285–2289; *Angew. Chem.* **2015**, *127*, 2314–2319.
[33] N. Buffet, E. Grelet, H. Bock, *Chem. Eur. J.* **2010**, *16*, 5549–5553.

[34] O. Guillermet, M. Mossoyan-Déneux, M. Giorgi, A. Glachant, J. C. Mossoyan, *Thin Solid Films* **2006**, *514*, 25–32.
[35] E. Clar, *The aromatic sextet*, Wiley, London **1972**.
[36] a) I. Gutman, I. Agranat, *Polycyclic Aromat. Compd.* **2006**, *2*, 63–73, 58; b) M. Solà, *Front. Chem.* **2013**, *1*, 22.
[37] T. Sakurai, T. Nakazato, H. Shinokubo, Y. Miyake, *Org. Lett.* **2021**, *23*, 2099–2103.
[38] a) Bruker, **2012**, Bruker AXS Inc.: Madison, Wisconsin, USA; b) STOE X-Area, **2016**, STOE & Cie: Darmstadt, Germany.
[39] G. M. Sheldrick, *Acta Crystallogr. Sect. A* **2015**, *71*, 3–8.
[40] G. M. Sheldrick, *Acta Crystallogr. Sect. C* **2015**, *71*, 3–8.
[41] A. L. Spek, *Acta Crystallogr. Sect. D* **2009**, *65*, 148–155.
[42] L. Farrugia, *J. Appl. Crystallogr.* **2012**, *45*, 849–854.

Manuscript received: May 14, 2021
Accepted manuscript online: June 28, 2021
Version of record online: July 22, 2021

